

## Photoluminescence pressure coefficients of InAs/GaAs quantum dots

Jun-Wei Luo, Shu-Shen Li, and Jian-Bai Xia

State Key Laboratory for Superlattices and Microstructures, Institute of Semiconductors, Chinese Academy of Sciences, P.O. Box 912, Beijing 100083, People's Republic of China

Lin-Wang Wang\*

Computational Research Division, Lawrence Berkeley National Laboratory, Berkeley, California 94720, USA

(Received 10 March 2005; published 21 June 2005)

We have investigated the ground exciton energy pressure coefficients of self-assembled InAs/GaAs quantum dots by calculating 21 systems with different quantum dot shape, size, and alloying profile using the atomistic empirical pseudopotential method. Our results confirm the experimentally observed significant reductions of the exciton energy pressure coefficients from the bulk values. We show that the nonlinear pressure coefficients of the bulk InAs and GaAs are responsible for these reductions, and the percentage of the electron wave function on top of GaAs atoms is responsible for the variation of this reduction. We also find a pressure coefficient versus exciton energy relationship which agrees quantitatively with the experimental results. We find linear relationships which can be used to get the information of the electron wave functions from exciton energy pressure coefficient measurements.

DOI: 10.1103/PhysRevB.71.245315

PACS number(s): 73.22.-f, 71.15.Dx, 81.40.Vw

### I. INTRODUCTION

Self-assembled InAs quantum dots (QDs) grown on lattice-mismatched GaAs(100) substrates have been studied extensively in both experiment and theory in the past 15 years due to their potential applications and matured synthesis processes.<sup>1</sup> Depending on synthesis methods and conditions, the quantum dot can have a different size, shape, and alloy profile. A major task of the research is to study the dependence of the electronic structure on the size, shape, and alloy profile. The electronic structure includes the electron wave functions and their eigenenergies. While there are many experimental ways to probe the electron eigenenergies and their confinement effects, it is much more difficult to experimentally measure the electronic wave functions. Thus any information about the electron wave functions will be extremely useful.

One recent popular experimental approach to study the electronic structure of a QD is to measure their pressure dependences of the photoluminescence (PL) energies. While the PL pressure coefficients (PC) for both bulk InAs and GaAs are close to 110 meV/GPa, it is found experimentally that the PL pressure coefficients for the quantum dots are usually much smaller and they can vary significantly from 60 to 100 meV/GPa,<sup>2-7</sup> depending on the samples. While Ma *et al.*<sup>2</sup> attributed the main reason for the much smaller PC to the built-in strain in InAs dots under nonlinear elasticity theory, Mintairov *et al.*<sup>9</sup> emphasized the nonuniform In distribution in QDs. There are also considerations for using the pressure dependence of the effective masses and confinement potentials to explain this reduction.<sup>2,4</sup> Manjón *et al.*<sup>3</sup> believed the PC is relevant to the penetration of the exciton wave function into the barrier by comparing different samples. But so far no quantitative agreements have been achieved between the model calculations and the experiment.

In this paper, via accurate atomistic calculations for the electron wave functions for these quantum dots, we have

revealed two facts: (i) The nonlinear elasticity and the nonlinear band-gap pressure dependence are responsible to the reduction of PC, and the variation of this PC reduction for different systems is mainly due to the different percentage of the electron wave function residing on top of InAs (or say GaAs) atoms (in the existence of alloys, this percentage is different from the percentage inside the QD region). (ii) There is a simple linear relationship between the value of the PC and the percentage of the electron wave function on top of GaAs; as a result it can be used as a way to probe the electron state properties from high-pressure experiments.

Note that the physical picture we obtained for the PC reduction is very different from previous considerations.<sup>2,4,9</sup> Although nonlinear elasticity and nonlinear band-gap pressure dependence were often considered and attributed to the reduction of PC, a simple particle-in-a-box picture was usually used in all the previous models (see, for example, Refs. 2,4,9), which assumes that the electron and hole states reside entirely inside the InAs QD. As a result, the observed large PC variations can only come from the different quantum confinement pressure dependence. Here we point out that this picture is wrong, and it is essential to consider the fact that a large portion (percentage) of the electron wave function is outside the InAs region, and this penetration is directly related to the variation of the PC reduction. The quantum confinement effect contributes less than 20% to the variation of the PC reduction. For the smallest QD we considered, the wave function outside the QD could be as large as 98% (although it is still a bound state).

### II. DETAILS OF CALCULATION

We will use the empirical pseudopotential method (EPM) (Ref. 10) to describe the single electron wave functions  $\psi_i(\mathbf{r})$  of an InAs quantum dot embedded in a GaAs matrix:

$$\left(-\frac{1}{2}\nabla^2 + V(\mathbf{r}) + V_{\text{NL}}\right)\psi_i(\mathbf{r}) = E_i\psi_i(\mathbf{r}), \quad (1)$$

here the total potential  $V(\mathbf{r})$  of the system is a direct sum of the screened atomic empirical pseudopotentials  $\nu_\alpha(r)$  of the constituent atoms (type  $\alpha$ ), and  $V_{\text{NL}}$  is the nonlocal potential describing the spin-orbit interaction. The plane-wave EPM approach has been used to study InAs and GaAs systems extensively, including quantum dots and alloys. The EPM is fitted to experimental band structures and deformation potentials; its results agree well with experiments for quantum well and quantum dots.<sup>11</sup> To study various quantum dots in our problem, we need computational supercells containing up to one million atoms. To solve Eq. (1) for these large systems, we have used the strained linear combination of bulk band (SLCBB) method.<sup>12</sup> In this method, the wave function  $\psi_i(\mathbf{r})$  is expanded by bulk Bloch states (which is in turn expanded by plane waves). Because the bulk Bloch states are good physical basis functions for the quantum dot states, we can truncate this basis set (down to 10 000) using physical intuition (e.g., selecting  $k$  points around the  $\Gamma$  point and bulk bands relevant to the quantum dot states) without introducing significant errors. The errors caused by the SLCBB method are around 10 meV near the band gap compared with the exact solution of Eq. (1).<sup>13</sup> Note that the absolute error of Eq. (1) compared to experiment is probably in the range of 50 meV, which is determined by the fitting of our EPM and the transferability of the EPM to the QD system. Nevertheless, the current approach is a much more accurate method compared to other traditional approaches like the  $\mathbf{k}\cdot\mathbf{p}$  method, where a few hundred meV error is possible.<sup>13</sup> The details of the SLCBB method and the selection of the bulk band basis and their effects were reported in Refs. 11,12.

To study the pressure effects on the electronic wave function, we first need to study the lattice relaxation under the pressure. We have used the Keating's valence force field (VFF) (Refs. 14 and 15) to describe the atomic relaxation. We have included bond-stretching, bond-bending, and bond-angle coupling interactions and high-order bond-stretching terms.<sup>11</sup> As a result, all the bulk moduli and the pressure dependence of the Young's moduli can be fitted exactly to the experimental values, and the VFF model describes correctly the atomic relaxations (e.g., near the InAs/GaAs surface) compared with total-energy *ab initio* results.<sup>11</sup> To be able to describe correctly the nonlinear lattice relaxation is important because there is a  $\sim 7.2\%$  lattice mismatch between bulk InAs and GaAs.

After the atomic relaxation is described by the VFF model, the pressure dependence of the bulk band structures for GaAs and InAs is described by the EPM Hamiltonian. Here, an explicit local strain dependence of  $\nu_\alpha(r)$  is used to describe the deformation potentials of the band energies.<sup>11</sup> Thus the fitting of  $\nu_\alpha(r)$  not only provides a correct band structure at zero pressure, it also provides correct high-order pressure dependence of the band energies. Figure 1 shows the calculated band energy pressure dependence for bulk InAs and GaAs. The calculated band-gap pressure coefficients for InAs and GaAs are 117 and 103 meV/GPa respec-

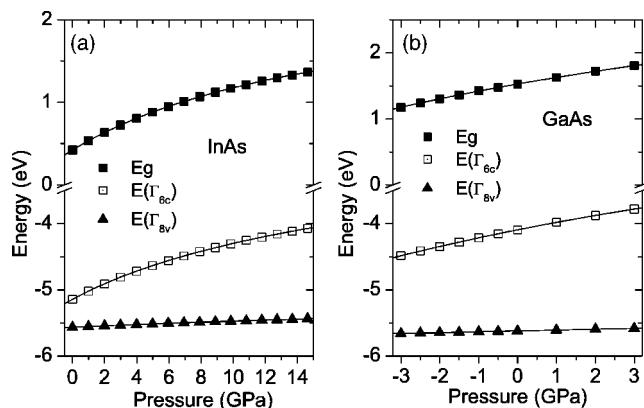


FIG. 1. The band-edge energies [ $E(\Gamma_{6c})$  and  $E(\Gamma_{8v})$ ] of (a) bulk InAs and (b) GaAs and their direct band gap  $E_g(\Gamma_{8v}-\Gamma_{6c})$  under hydrostatic pressure.

tively, they agree well with the experimental values of 114 and 106(4) meV/GPa.<sup>16</sup>

We next use the above VFF and EPM Hamiltonians to calculate various embedded quantum dots under different pressures. A large variety of QD shapes have been reported and studied for the InAs/GaAs system by various groups, for example, pyramidal quantum dot (PQD) with side facets oriented along  $\{101\}$ ,  $\{113\}$ , or  $\{105\}$ ,<sup>17</sup> or truncated pyramidal quantum dot (TPQD).<sup>18,19</sup> Inside the QD, various In/Ga profiles have been speculated, for example, an inverted-triangle shape In-rich core<sup>19</sup> or a growth direction linearly increasing In concentration.<sup>18</sup> To cover the whole spectrum of possible shapes and alloy profiles, we have calculated 21 QDs as shown in Table I. Their geometries, sizes, and compositions are chosen before any calculations. They are: eight pure InAs pyramidal quantum dots (PQDs) with  $\{101\}$  or  $\{113\}$  facets and base sizes of 6, 9, 11.3, and 15 nm; three PQDs with  $\{105\}$  facets and base sizes of 11.3, 15, and 20 nm; three truncated pure InAs pyramidal QDs (TPQDs) with  $\{101\}$  facets, 8 nm base size, and height/base ratios of 2/3, 1/2, and 1/4; 5 TPQDs with  $\{101\}$  facets, 11.3 nm base size, and height/base ratios of 2/3, 1/2, 1/4, 1/5, 1/10; two alloy pyramidal QDs with  $\{101\}$  facets, 11.3 nm base size, and bottom Ga percentages of 40% and 50% (zero Ga percentage at the tip). To distinguish these 21 QDs, they are numerated from 1 to 21 as in Table I. In the following Figs. 2–4 the digits in the open squares correspond to their numbers in Table I.

The above described InAs quantum dots are embedded in a pure GaAs matrix. A supercell box is used to contain the quantum dot. A periodic boundary condition is used for the supercell box. To remove the possible dot-dot electronic and elastic interactions, a sufficient GaAs barrier is used. As a result, a supercell can contain up to one million atoms. The atomic positions within the supercell are then relaxed by minimizing the strain energy of the VFF Hamiltonian. To create a pressure, the overall size of the supercell is changed, and the pressure is calculated from the local GaAs strains away from the quantum dot. After the atomic positions are relaxed, the electron and hole eigenstates and eigenenergies of Eq. (1) are solved using the SLCBB method.

TABLE I. The 21 calculated quantum dots.

Pure InAs pyramidal quantum dots (PQDs)													
	1	2	3	4	5	6	7	8	9	10	11		
Facet	{101}	{101}	{101}	{101}	{113}	{113}	{113}	{113}	{105}	{105}	{105}		
Base size (nm)	6	9	11.3	15	6	9	11.3	15	11.3	15	20		
Pure InAs truncated pyramidal quantum dots (TPQDs)													
	12	13	14	15	16	17	18	19					
Facet	{101}	{101}	{101}	{101}	{101}	{101}	{101}	{101}					
Base size (nm)	6	6	6	11.3	11.3	11.3	11.3	11.3					
Height/base	2/3	1/2	1/4	2/3	1/2	1/4	1/5	1/10					
Alloy pyramidal quantum dots													
					20					21			
Facet					{101}					{101}			
Base size (nm)					11.3					11.3			
Alloy profile					bottom 40%Ga, tip 0%Ga					bottom 50%Ga, tip 0%Ga			

### III. RESULTS AND DISCUSSION

We typically calculate five pressure values from 0 to 2 GPa for each quantum dot. Using these five points, the ground exciton energy of the quantum dot is fitted as  $E_g(P) = E_g(0) + a_1P + a_2P^2$ . Then the linear pressure coefficients (PCs) of the exciton energy is read out from  $a_1$ . Consistent with the experiment, we find that this PC is in the range of 60–110 meV/GPa, much smaller than the bulk InAs and GaAs PCs. We then plot all the calculated PCs as a function of the QD zero-pressure exciton energy  $E_0(0)$  in Fig. 2. Note that the QD exciton energy  $E_0(0)$  is the single-particle energy gap between the lowest electron state and the highest hole state minus the screened Coulomb interaction

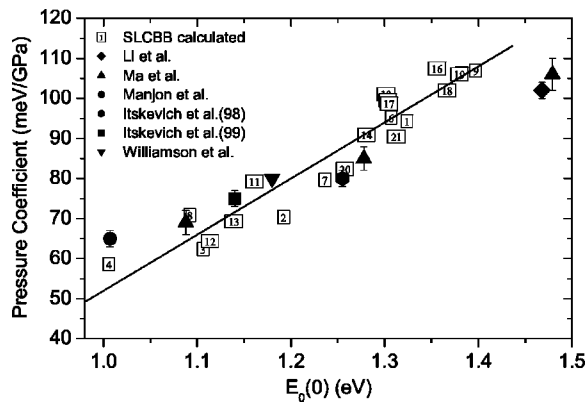


FIG. 2. The PL pressure coefficient ( $E'_0$ ) vs  $E_0(0)$  (PL energy) and comparison with experiments. The  $E_0(0)$  is the zero-pressure exciton energy which equals the single-particle electron-hole gap minus the electron-hole Coulomb interaction. The experimental results are Li *et al.* (Ref. 7), Ma *et al.* (Ref. 2), Manjon *et al.* (Ref. 3), and Itskevich *et al.* (Refs. 5 and 6). We also included one previously calculated result from Williamson *et al.* (Ref. 8).

between the electron and the hole, as described in Ref. 11. This Coulomb interaction is the same as in the Bethe-Salpeter equation, although we only used a single electron-hole configuration. Since the confinement in a QD is mainly caused by the potential well, not by the Coulomb interaction, the multiconfiguration effects are very small, they only amount to a few meV,<sup>20</sup> while the single configuration electron-hole Coulomb interaction is in the range of a few tens meV. Surprisingly, despite all the different shapes and sizes for the 21 QDs we studied, we find a rough linear relationship between the PC and the exciton energies for all the systems we calculated. This provides a convenient way to compare with the experiment, without the need to know the QD sizes and shapes which are not available from the experiment. The theory and experiment comparison is shown in Fig. 2. The agreement is excellent considering all the possible uncertainties involved. We see that, indeed, the QD pressure coefficients are much smaller than the bulk values of both InAs and GaAs, and they increase with the exciton energy.

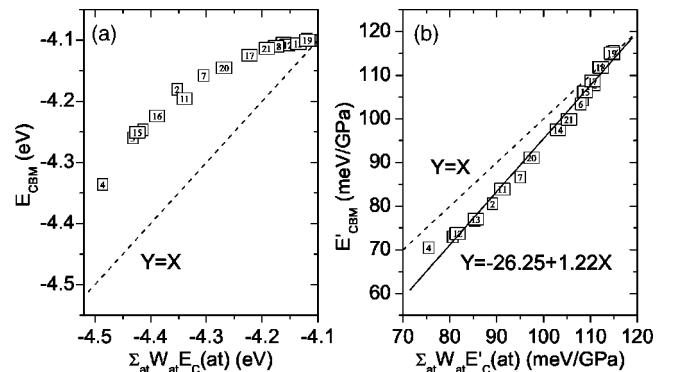


FIG. 3. (a)  $E_{\text{CBM}}$  as a function of  $\sum_{\text{at}} W_{\text{at}} E'_c(\text{at})$ ; (b)  $E'_{\text{CBM}}$  as a function of  $\sum_{\text{at}} W_{\text{at}} E'_c(\text{at})$ .

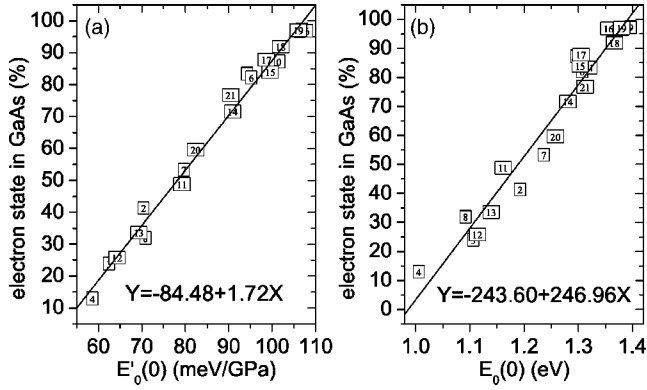


FIG. 4. (a) The relationship between  $E'_0(0)$  and  $x$  (the percentage of the electron state in GaAs); (b) the relationship between  $E_0(0)$  and  $x$ .

To understand the variation of the PC, and its dependence on the QD, we can perform a simple analysis. We will concentrate on the conduction-band minimum (CBM) state since most of the band-gap pressure coefficient comes from the conduction band.<sup>21</sup> For a simple approximation, we can express the energy  $E_{\text{CBM}}$  of the CBM eigenstate  $\psi_{\text{CBM}}(\mathbf{r})$  as a sum of an effective mass like potential energy and a kinetic energy  $E_k$ .<sup>22</sup> The potential energy can be approximated by a weighted sum of the local conduction-band energy, then we have

$$E_{\text{CBM}} \approx \int |\psi_{\text{CBM}}(\mathbf{r})|^2 E_c(\mathbf{r}) d^3\mathbf{r} + E_k; \quad (2)$$

here the  $E_c(\mathbf{r})$  is the bulk conduction-band energy for the given local strain at  $\mathbf{r}$  and the local constituent material (either GaAs or InAs). Note that, in practice, the spatial integral of Eq. (2) is replaced by a sum over the atom  $\sum_{\text{at}} W_{\text{at}} E_c(\text{at})$ , where the local strain for an atom is calculated from the atom's nearest-neighbor atomic positions, and  $W_{\text{at}}$  denotes the weight of  $|\psi_{\text{CBM}}(\mathbf{r})|^2$  at that atom "at." We have plotted the SLCBB calculated  $E_{\text{CBM}}$  as a function of  $\sum_{\text{at}} W_{\text{at}} E_c(\text{at})$  in Fig. 3(a). We see that all the calculated QDs fall into a nice curve. The difference between this curve and the dashed line (the potential-energy line) is the kinetic energy  $E_k$ .

Now, we analyze the pressure coefficients of  $E_{\text{CBM}}$  using Eq. (2). If we ignore the pressure dependences of the kinetic energy and the weight function  $W_{\text{at}}$ , we can have an approximated relationship:

$$E'_{\text{CBM}} \approx \int |\psi_{\text{CBM}}(\mathbf{r})|^2 E'_c(\mathbf{r}) d^3\mathbf{r}; \quad (3)$$

here the prime indicates the derivation with pressure. Despite all the approximations, the left- and right-hand side of Eq. (3) do form a rough linear relationship, as shown in Fig. 3(b). Nevertheless, the left- and the right-hand side of Eq. (3) are not exactly the same. This is shown in Fig. 3(b) by the  $y=x$  dashed line, which is slightly above the actual  $E'_{\text{CBM}}$ . The difference should come from the pressure dependence of the  $E_k$  in Eq. (2). From Fig. 3(b), we see that the kinetic energy term (which is the confinement energy in a simple

particle-in-a-box picture with infinite wall) contributes less than 20% of the total PC reduction. The majority of PC reduction comes from the right-hand side of Eq. (3), which as we will state below is mainly determined by the percentage of the electron on top of the GaAs atoms.

The physical meaning of Eq. (3) is clear and useful [especially when it is written as  $E'_{\text{CBM}} \approx \sum_{\text{at}} W_{\text{at}} E'_c(\text{at})$ ]: the PC of the quantum dot state is a wave-function weighted sum of the local PC at all the atoms. The  $E'_c(\text{at})$  depends on the local strain of this atom as illustrated in Fig. 1. This can be used to understand why the QD PC is in general less than the bulk InAs and GaAs results. Because InAs in the QD is always under compressive strain, due to the nonlinear PC as shown in Fig. 1 (which originates from nonlinear elasticity<sup>23</sup>), the  $E'_c$  in the InAs region is significantly smaller than its bulk value. On the other hand, GaAs is under tensile strain, which will increase  $E'_c$ . Because the magnitude of the GaAs strain is in general smaller than the InAs strain, and because most of the wave function is localized in the InAs region if the quantum dot is not too small, the averaged PC is then smaller than the bulk InAs and GaAs PCs. However, when the majority of the wave function is inside GaAs, it is possible that the QD state PC is actually larger than the bulk GaAs PC (since GaAs is under tensile strain). This is true for the smallest quantum dot we calculated, where 98% of the wave function is inside GaAs, and the calculated QD PC ( $\sim 106$  meV/GPa) as shown in Fig. 4(a) is slightly larger than the GaAs bulk value of 103 meV/GPa. In conclusion, it is essential to take into account the penetration of the electron wave function into the GaAs barrier in order to understand the variation of the PC reductions in the QDs. This is contrary to most of the current models used in this field.

Guided by Eqs. (2) and (3), we now try to find some simple relationships between the experimentally easily observable quantities (exciton energy and pressure coefficients) and the wave-function properties. In Eq. (3), if we approximate  $E'_c(\text{at})$  by just two values, one for InAs, one for GaAs, then  $E'_{\text{CBM}}$  of Eq. (3) becomes a linear function of  $x = \sum_{\text{at} \in \text{GaAs}} W_{\text{at}} / \sum_{\text{at} \in \text{all}} W_{\text{at}}$  (i.e., the percentage of the wave function on top of GaAs). This is tested in Fig. 4(a) (where we have plotted the pressure coefficients of the exciton energy, not just the CBM energy, so the connection with experiment is more straightforward). We see that  $E'_0$  and  $x$  form a very nice straight line. This can be very useful, since a measured  $E'_0$  value will give us the  $x$ , which is a property of the wave function that cannot be measured directly by other means. The same relationship can be plotted between the exciton energy itself,  $E_0$ , and the  $x$ , as in Fig. 4(b). They also form a rough linear relationship with slightly larger scatters. This is what we found numerically within the range of systems we have considered. Although these linear relationships might not be exact, from a practical point of view, they can be very useful. The linear relationships in Figs. 4(a) and 4(b), in turn, explain why we have a roughly approximated linear relationship between  $E'_0$  and  $E_0$  in Fig. 2. This is because both  $E'_0$  and  $E_0$  are linearly correlated with  $x$ .

#### IV. CONCLUSION

In summary, using accurate and reliable empirical pseudo-potential methods and the SLCBB calculations, we have

studied InAs and GaAs quantum-dot PL pressure coefficients. We investigated 21 different quantum dots covering the ranges of experimental QD size, shape, and alloy profile. We found linear relationships between PC and exciton energy, which agree excellently with the experimental results. We point out that it is necessary to consider the penetration of the electron state into the GaAs barrier in order to understand the PC reductions and their large variations. We find various relationships between the pressure coefficients and the exciton energies, and the electronic wave-function properties. Especially, we find linear relationships between the wave-function percentage on top of GaAs and the PL pressure coefficients and PL energies. These relationships can be

used to obtain the information of the electron states via the measurements of PC or the exciton energy energies.

#### ACKNOWLEDGMENTS

We would like to acknowledge G. H. Li and B. S. Ma for helpful discussions. Part of the CPU- time of this work was supplied by Supercomputing Center, CNIC, CAS. This work was supported by the National Natural Science Foundation of China and the special funds for Major State Basic Research Project No. G2001CB309500 of China. The work by L. W. Wang was also funded by U.S. Department of Energy under Contract No. DE-AC03-76SF00098.

\*Electronic address: lwwang@lbl.gov

- <sup>1</sup>D. Bimberg, M. Grundmann, and N. N. Ledent, *Quantum Dot Heterostructures* (Wiley, New York, 1999), and references therein.
- <sup>2</sup>B. S. Ma, X. D. Wang, F. H. Su, Z. L. Fang, K. Ding, Z. C. Niu, and G. H. Li, *J. Appl. Phys.* **95**, 933 (2004).
- <sup>3</sup>F. J. Manjón, A. R. Goñi, K. Syassen, F. Heinrichsdorff, and C. Thomsen, *Phys. Status Solidi B* **235**, 496 (2003).
- <sup>4</sup>I. E. Itskevich, M. Henini, H. A. Carmona, L. Eaves, P. C. Main, D. K. Maude, and J. C. Portal, *Appl. Phys. Lett.* **70**, 505 (1997).
- <sup>5</sup>I. E. Itskevich, S. G. Lyapin, I. A. Troyan, P. C. Klipstein, L. Eaves, P. C. Main, and M. Henini, *Phys. Rev. B* **58**, R4250 (1998).
- <sup>6</sup>I. E. Itskevich, I. A. Trojan, S. G. Lyapin, M. J. Steer, L. R. Wilson, D. J. Mowbray, M. S. Skolnick, M. Hopkinson, L. Eaves, and P. C. Main, *Phys. Status Solidi B* **211**, 73 (1999).
- <sup>7</sup>G. H. Li, A. R. Goñi, K. Syassen, O. Brandt, and K. Ploog, *Phys. Rev. B* **50**, 18420 (1994).
- <sup>8</sup>A. J. Williamson and A. Zunger, *Phys. Rev. B* **58**, 6724 (1998).
- <sup>9</sup>A. M. Mintairov, K. Sun, J. L. Merz, C. Li, A. S. Vlasov, D. A. Vinokurov, O. V. Kovalenkov, V. Tokranov, and S. Oktyabrsky, *Phys. Rev. B* **69**, 155306 (2004).
- <sup>10</sup>L. W. Wang and A. Zunger, *Phys. Rev. B* **51**, 17398 (1995).
- <sup>11</sup>A. J. Williamson, L. W. Wang, and A. Zunger, *Phys. Rev. B* **62**, 12963 (2000).

- <sup>12</sup>L. W. Wang and A. Zunger, *Phys. Rev. B* **59**, 15806 (1999).
- <sup>13</sup>L. W. Wang, A. J. Williamson, and Alex Zunger, *Appl. Phys. Lett.* **76**, 339 (2000)
- <sup>14</sup>C. Pryor, J. Kim, L. W. Wang, A. J. Williamson, and A. Zunger, *J. Appl. Phys.* **83**, 2548 (1998).
- <sup>15</sup>P. N. Keating, *Phys. Rev.* **145**, 637 (1966).
- <sup>16</sup>Landolt Börnstein, *Numerical Data and Functional Relationships in Science and Technology*, Vol. 22, Subvol. a (Springer-Verlag, Berlin, 1987); see also Vol. 41, Subvol. A1A (Springer-Verlag, Berlin, 2001).
- <sup>17</sup>J. Kim, L. W. Wang, and A. Zunger, *Phys. Rev. B* **57**, R9408 (1998), and references therein.
- <sup>18</sup>D. M. Bruls, J. W. A. M. Vugs, P. M. Koenraad, M. S. Skolnick, M. Hopkinson, F. Long, S. P. A. Gill, and J. H. Wolter, *Appl. Phys. Lett.* **81**, 1708 (2002).
- <sup>19</sup>N. Liu, J. Tersoff, O. Baklenov, A. L. Holmes, Jr., and C. K. Shih, *Phys. Rev. Lett.* **84**, 334 (2000).
- <sup>20</sup>J. Shumway, A. Franceschetti, and A. Zunger, *Phys. Rev. B* **63**, 155316 (2001).
- <sup>21</sup>S. H. Wei and A. Zunger, *Phys. Rev. B* **60**, 5404 (1999).
- <sup>22</sup>G. Bastard, *Wave Mechanics Applied to Semiconductor Heterostructures* (Halsted Press, New York, 1988).
- <sup>23</sup>M. D. Frogley, J. R. Downes, and D. J. Dunstan, *Phys. Rev. B* **62**, 13612 (2000).